AJNR

Intracranial Chemical-Shift Artifacts on MR Images of the Brain: Observations and Relation to Sampling Bandwidth

Alison S. Smith, Meredith A. Weinstein, Gregory C. Hurst, Dale R. DeRemer, Richard A. Cole and Paul M. Duchesneau

AJNR Am J Neuroradiol 1990, 11 (2) 303-311
http://www.ajnr.org/content/11/2/303

Intracranial Chemical-Shift Artifacts on MR Images of the Brain: Observations and Relation to Sampling Bandwidth

Alison S. Smith[1,2]
Meredith A. Weinstein[3]
Gregory C. Hurst[1]
Dale R. DeRemer[3]
Richard A. Cole[4]
Paul M. Duchesneau[3]

The purpose of this study was to evaluate the presence of chemical-shift artifacts on cranial MR and to illustrate the interrelationship among chemical-shift artifacts, variable acquisition parameters, and field strength. Measurements of chemical-shift artifacts were performed on scans obtained from a volunteer imaged in a 1.5-T General Electric system at bandwidths of 8, 16, and 32 kHz, using a 24-cm field of view and an 8-kHz bandwidth with a 48-cm field of view. Chemical-shift displacements at 8 kHz were 6.6 and 14.2 mm at the respective fields of view. Retrospective review was also performed in 77 cases of cranial MR performed on a 1.4-T Technicare unit for the presence and source of chemical-shift artifact on spin-density and T2-weighted images. Most data reviewed showed no significant interference of chemical-shift artifacts on cranial images. An artifactual subdural fluid collection was a common artifact (n = 30/77). When present, this was due to shift of fat signal from subcutaneous tissues onto the brain in patients younger than 10 years old (n = 4/10) and correlated with the distance between brain and subcutaneous fat of less than the linear value of the chemical shift. When this artifact was present in adults (n = 25/67), it was due to shift of the medullary fat signal across the inner table of the skull. The latter also occurred in one child under 10. Apparent location shifts, consistent with the displacement expected from the chemical-shift artifact, were noted in five of five cases of intracranial lipoma. In one of these, the chemical-shift artifact disguised the presence of a large associated vessel. The method of calculating the linear displacement of chemical-shift artifact is reviewed, and the interrelationship of machine parameters and chemical-shift artifact is illustrated. Chemical-shift artifact increases proportionally with field strength and field of view. Increasing the bandwidth to decrease chemical-shift artifact has a resultant penalty in signal to noise but allows a lower time to echo. A lower time to echo can also be accomplished without increasing the bandwidth if asymmetric sampling is used.

Awareness of the relationships among chemical-shift artifacts, acquisition parameters, and field strengths can result in a more tailored examination when the chemical-shift artifact is going to be a significant factor. In addition, interpreter error can be avoided by awareness of these relationships when reviewing images from outside institutions.

***AJNR* 1990:303–311, March/April 1990; *AJR* 154: June 1990**

Received January 19, 1989; revision requested March 31, 1989; revision received September 7, 1989; accepted September 22, 1989.

[1] Department of Radiology, Cleveland Metropolitan General Hospital, Cleveland, OH 44109.

[2] Present address: Department of Radiology, University Hospitals of Cleveland, 2074 Abington Rd., Cleveland, OH 44106. Address reprint requests to A. S. Smith.

[3] Department of Radiology, Neuroradiology Section, Cleveland Clinic Foundation, Cleveland, OH 44106.

[4] Division of Research, Cleveland Clinic Foundation, Cleveland, OH 44106.

0195–6108/90/1102–0303

We observed that the chemical-shift artifacts causing apparent subdural hematomas were seen frequently on a Technicare 1.4-T Teslacon system and seen infrequently on General Electric 1.5-T Signa, Picker 1.5-T Vista, Technicare 0.6-T Teslacon II, and Picker 0.5-T Vista systems. We further observed that with the Technicare 1.4-T system, these apparent subdural hematomas were common in the first decade of life, less common between the ages of 10 and 39, and more common over the age of 40. The current study was performed to determine (1) what patient variables contribute to chemical-shift artifacts that mimic subdural hematomas; (2) which MR parameters contribute to these artifacts; and (3) what the relationships are among these parameters.

Theory of Chemical Shift

The basis of chemical-shift artifact, chemical-shift imaging, and clinical-shift spectroscopy is the variation of the local magnetic field (nuclear environment) due to the magnetic moment of electrons near the nucleus of interest. If this electronic magnetic field opposes the main (applied) magnetic field, as in the vast majority of human tissues [1, 2], the effective local magnetic field is "shielded" so that nuclei in this environment experience a field less than that of the applied magnetic field. The net contribution of these distortions of the applied magnetic field is measured by diamagnetic susceptibility [3–5]. Paramagnetic effects are due to the "extra" magnetic field produced by electrons; this field augments rather than opposes the applied field, but due to molecular dynamics the principal observed effect of paramagnetism is shortened T1 and T2 relaxation times.

Hydrogen molecules bound to fat will precess at a slightly slower rate than hydrogen molecules of water because they are more shielded from the applied magnetic field and therefore experience a lower magnetic field. Because the MR system translates a received signal at a given frequency to a specific predictable location on the image, when the gradient field is applied during the "readout" mode of the imaging cycle, these fat protons will appear at a lower frequency. This "frequency misregistration," or "chemical-shift" artifact, results in a position shift (displacement) of fat signal relative to signal from water at the same physical location. This effect is most obvious on the MR image when a tissue containing predominantly fat is sharply interfaced with one that is predominantly of water content.

Chemical-shift artifact is directly proportional to the field strength because the frequency difference increases as the Larmor frequency increases. As can be seen in Figure 1, the steeper the gradient, the less the distance that the fat signal is displaced relative to the water signal. If the receiver bandwidth is doubled and the gradient is doubled to keep the same resolution and field of view (FOV), the chemical shift will be one-half as great. If the FOV in the frequency-encode direction is doubled, and resolution hence reduced by half, the gradient will be half as steep and the distance of the chemical-shift artifact will be twice as large. Because the fat signal is at a lower frequency, it appears on the image to be shifted in the lower field direction "downfield" of the gradient, relative to the water signal. The overlap of the fat signal with adjacent tissue can result in an artifact of extra, displaced signal, while the loss of signal from the fat at the original site results in a signal void at this location. The location of the chemical-shift artifact on the image can be changed by reorienting the frequency-encode axis or by reversing the gradient.

Bandwidth

For the purposes of this discussion, bandwidth will refer to either "signal" or "receiver" frequency ranges. The strength of the frequency-encoded gradient determines the range of frequencies contained in the image data signal. This range of frequencies is called the signal bandwidth. An increase in the signal bandwidth requires an equal increase in the system receiver sampling bandwidth to accommodate the greater range of signal frequencies. This is obtained by decreasing (narrowing) the time used for data collection (sampling). Steeper gradients result in a wider frequency bandwidth per pixel; therefore, the variance in fat and water signals are less significant, as shown in Figure 1.

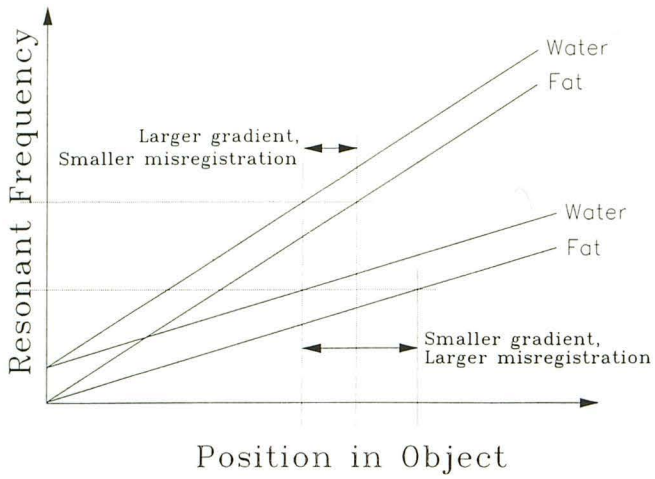

Fig. 1.—Because of different chemical shifts, water and fat in same external field will resonate at slightly different Larmor frequencies. In the presence of a spatially encoding field gradient, resonant frequency will depend on *both* position and chemical shift. Thus, water and fat at different positions will appear to be in the same place since they will have the same frequency. Position in the image is determined directly from resonant frequency, so that fat and water will be misregistered in the image. As gradient strength becomes smaller, this misregistration becomes larger; fat and water, which are farther apart in the subject, will have the same frequency, and hence be mapped to the same spot in the image.

Materials and Methods

With the use of the General Electric 1.5-T system, a 67-year-old volunteer was examined at bandwidths of 32, 16, and 8 kHz with a 24-cm FOV and at an 8-kHz bandwidth with a 48-cm FOV. Comparisons were made of measured vs calculated chemical-shift artifacts. The default and user-selectable sampling bandwidth and the minimum time to echo (TE) attainable with these bandwidths were determined for Technicare 0.6-T Teslacon II and 1.4-T Teslacon I, General Electric 1.5-T Signa, and Picker International 0.5-T and 1.5-T Vista systems.

Retrospective evaluation was made in 77 consecutive patient studies performed on a 1.4-T Teslacon I unit using a 25.6-cm FOV, 256 (x or frequency-encode) by 192 (y or phase-encode) matrix, 16.6-kHz sampling bandwidth, and frequency gradient strength of 0.1529 g/cm. Spin-echo images were obtained in axial and/or coronal planes using spin-density, 2010/32 (TR/TE), and T2-weighted, 2010/120, sequences. The frequency-encoding (x) axis was left-to-right in both planes with the gradient producing a higher field to the right. Qualitative assessment was made of the presence of chemical-shift artifacts at interfaces of fat and water. The presence of these artifacts was related to age, average skull thickness for age as determined by Orley [6], and measured biparietal diameter (BPD). BPD was measured at the level of the thalami. The presence of artifactual subdural fluid collections was correlated with these age groupings by decade. Quantitative linear measurements were made on the images after

comparing magnification factors with cursor measurements on the imaging unit. Measurements were also made of shift artifacts seen in five cases of known intracranial lipomas, four studied with the 1.4-T Technicare system and one with the 1.5-T General Electric system (gradient strength = 0.31 g/cm). CT examinations in these cases were compared with the MR images for evaluation of the presence of calcifications, associated vessels, and apparent position change of the lipoma when compared with the MR images.

Results

Images in the volunteer obtained at a 24-cm FOV with progressive sampling bandwidths of 8, 16, and 32 kHz showed measured linear chemical-shift artifacts of 6.6, 3.8, and 1.9 mm compared with calculated values of 6.7, 3.4, and 1.7 mm, respectively (Fig. 1). Doubling the FOV from 24 to 48 cm at an 8-kHz bandwidth resulted in measured shifts of 6.6 and 14.2 mm compared with calculated values of 6.7 and 13.4 mm, respectively. Because it was difficult to define the edges of the artifact at a 48-cm FOV, the value is the mean of five measurements. Table 1 lists the default and selectable receiver bandwidths for the MR systems studied. Also listed are the minimal TEs attainable with these bandwidths.

On the 1.4-T Teslacon I system, the calculated shift of signal between juxtaposed fat and water was 3.2 mm (3.2 pixels). Of the 77 patient studies reviewed, 52 were in females and 25 were in males. The patients were 9 months to 85 years old. Chemical-shift artifacts caused a relative asymmetry of the brain within the surrounding ring of subcutaneous and/or diploic fat signal in all studies. Most studies reviewed showed no subdural artifact. When this asymmetry resulted in an artifactual subdural fluid collection, it was due to shift of fat signal from the subcutaneous tissue in those under 10 years of age (Fig. 2) and to shift of fat signal of the diploic cavity onto the brain in older individuals (Fig. 3). Shift of the subcutaneous tissue onto the brain was not observed beyond the age of 8.

TABLE 1: Relationships Among Machine Parameters, Chemical-Shift Artifacts, and Sampling Bandwidths

Variable	Increased Bandwidth	Increased Field of View	Increased Field Strength
Chemical-shift artifact	Decreased	Increased	Increased
Signal to noise	Decreased	Increased	Increased
TE	Decreased	–	–

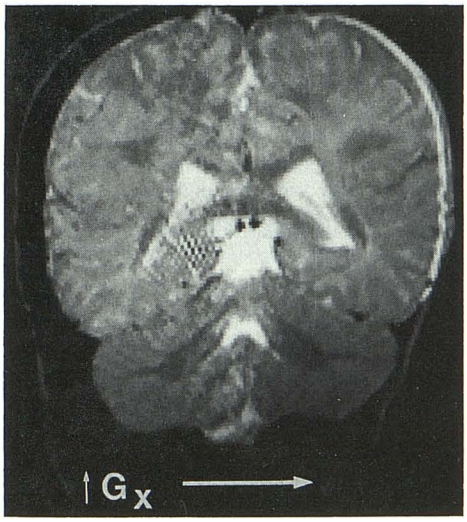

Fig. 2.—Overlap of brain with fat signal from subcutaneous tissue in this 1-year-old child results in artifactual subdural hematoma on 2000/120 image. Frequency encoding is left to right, with higher side of gradient to the right (G_x).

The presence of a subdural artifact from overlap of the diploic fat signal showed a generally increasing trend with increased age (see Fig. 4). The age differences between artifact groups that showed subdural effects due to subcutaneous tissue overlap vs no overlap and between subdural artifact due to shift of subcutaneous vs diploic fat signal were significant by the t test ($p = .0001$). The patients with a shift of the subcutaneous tissue onto the brain had an average BPD of 12.3 cm, patients with overlap of diploic fat signal had an average BPD of 14.2 cm, and patients who had no demonstrable overlap had an average BPD of 14.0 cm. The differences in BPD between the first two groups were significant by the t test ($p = .001$). Differences in BPDs between those having no artifact and overlap of the diploic fat signal were not significant.

Retrospective evaluation of the five cases of intracranial lipoma showed chemical-shift artifacts of 3–4 mm on the 1.4-T Technicare studies and approximately 2 mm on the 1.5-T General Electric examination. An area of decreased signal adjacent to these lipomas, representing the higher field direction of the gradient ("upfield") side of the artifact, had prospectively been called calcification or vessel in three of five cases. Calcification was not present in these sites on CT (Fig. 5). The downfield bright signal of the chemical-shift artifact obscured the presence of a large vessel adjacent to a sylvian fissure lipoma in one case (Fig. 6) and resulted in underestimation of calcification associated with a corpus callosum lipoma in another case.

Discussion

Relationship of Bandwidth to Chemical-Shift Artifacts and Other MR Parameters

Sampling bandwidth changes are related to the changes of strength of the read (x) gradient. The magnitude of the chemical-shift artifact depends on the effect of the inherent (chemical-shift) frequency difference between fat and water relative to the range of frequencies accountable to a given pixel. In other words, if the alteration of signal that occurs from the fat/water difference is small, relative to the range of signals expected in a given pixel, the chemical-shift artifact will not have a significant effect on the image (see Fig. 1). The amount of chemical shift can be determined by solving several simple equations. Needed values are FOV, bandwidth, and resonant frequency for the field strength of the MR unit.

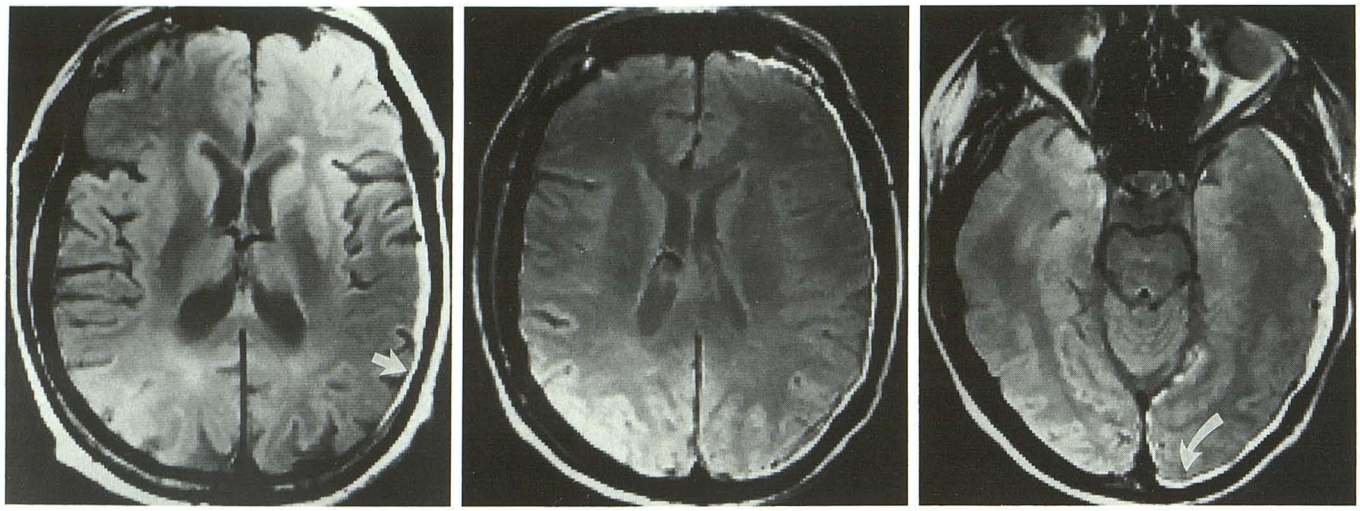

Fig. 3.—Rim of increased signal at left parietal cortex is evident in *A* and *B*.
***A*, Chemical-shift artifact from fat signal of diploic space has overlapped onto brain (*arrow*).**
***B* and *C*, Subdural hematoma is confirmed. Size of collection exceeds expected size of artifact, shows continuation of signal into posterior interhemispheric fissure, and does not taper at anterior and posterior poles where frequency-encoded artifact would be expected to diminish (*arrow*).**

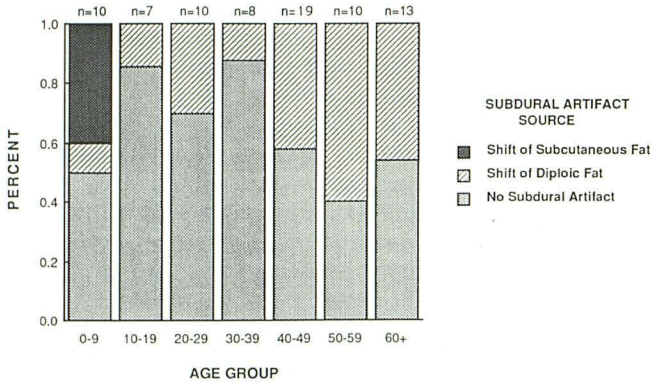

Fig. 4.—Artifact distribution within an age group.

Determine the frequency offset between fat and water in Hertz:

Frequency offset (ppm) = shift (Hz)/resonant frequency (MHz). (1)

By using 3.5 ppm as the average chemical shift between fat and water, at 1.5 T, 3.5 ppm = frequency shift/64 MHz (frequency shift = 224 Hz).

After selecting the bandwidth (i.e., 32 kHz) at a given FOV (24 cm), determine the expected offset distance:

Expected offset distance (mm) = [frequency shift (Hz) × FOV (mm)]/bandwidth (Hz)
= 224 Hz × 240 mm/32,000 Hz
= 1.68 mm. (2)

The linear displacement of the chemical-shift artifact is estimated at 1.68 mm in the frequency-encoded axis in this example. However, allowance for pixel size and measurement error must be considered. The frequency shift between fat and water is between 3.0 and 3.5 ppm. We arbitrarily chose 3.5 ppm as the value of the protons providing the majority of human "fat" signal.

The following conclusions can be made about chemical shift if only one variable is altered at a time in the formulas 1 and 2.

1. The distance of the chemical-shift artifact is directly proportional to the strength of the magnetic field. Doubling the magnetic field will double the chemical-shift measurement in Hertz and in millimeters (see equation 1).

2. The distance of the chemical-shift artifact is inversely proportional to the sampling bandwidth. Doubling the sampling bandwidth will double the steepness of the gradient (to maintain the same resolution) and halve the distance of the chemical shift, as shown in Table 2. At 24-cm FOV, the artifact at 8, 16, and 32 kHz by cursor measurement was less than 1 mm from the calculated values of 6.7, 3.4, and 1.7 mm, respectively (Fig. 7).

3. The distance of chemical-shift artifact is directly proportional to the FOV. Doubling the FOV will halve the gradient and double the amount of chemical shift (Table 2). Measured artifact at 8 kHz with 24- and 48-cm FOVs differed by a factor of two, but the value at 48-cm FOV is an estimate since there was difficulty defining the margins of the fat signal on this image (Fig. 7).

It is important for the radiologist operating the MR system to understand the effects of and interrelationships involved in altering the sampling bandwidth, so the bandwidth can be optimized for each examination. At a given magnetic field

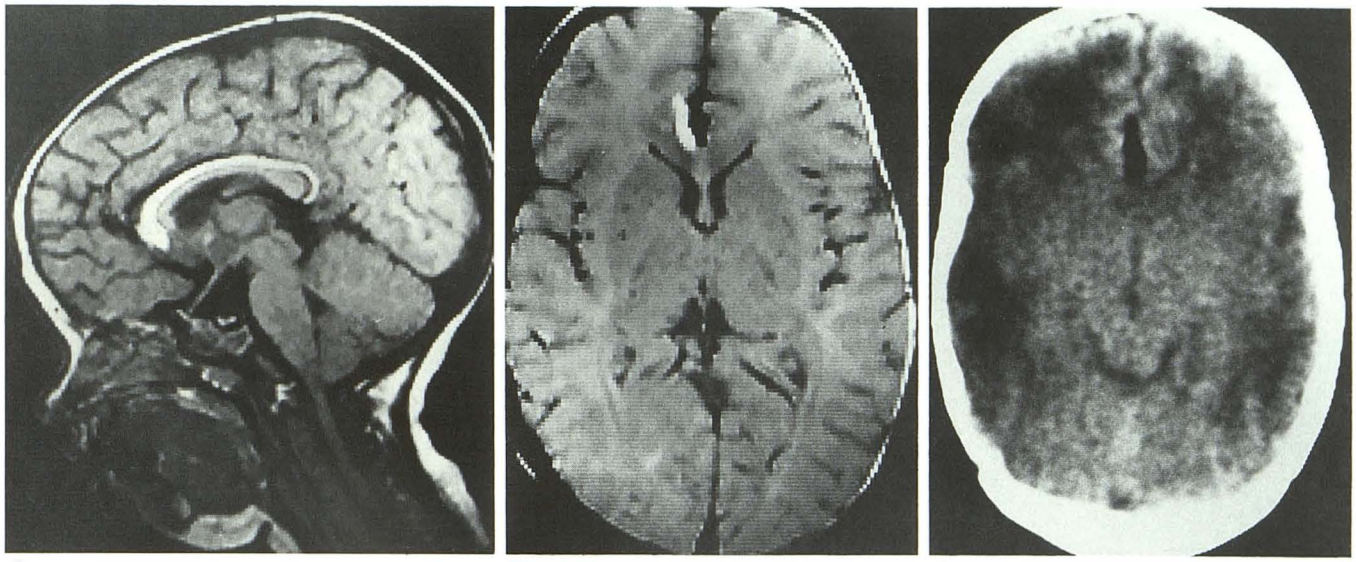

Fig. 5.—Fat signal in corpus callosum lipoma is superimposed on brain parenchyma by 3 mm, showing clinically insignificant but definite change from CT.

***A*, Sagittal image (500/30) shows downfield (right) shift of lipoma.**

***B*, Axial MR image shows lipoma overlapping frontal cortex on downfield (left) side of image.**

***C*, Axial CT scan indicates lipoma is closer to midline; there is no associated calcification.**

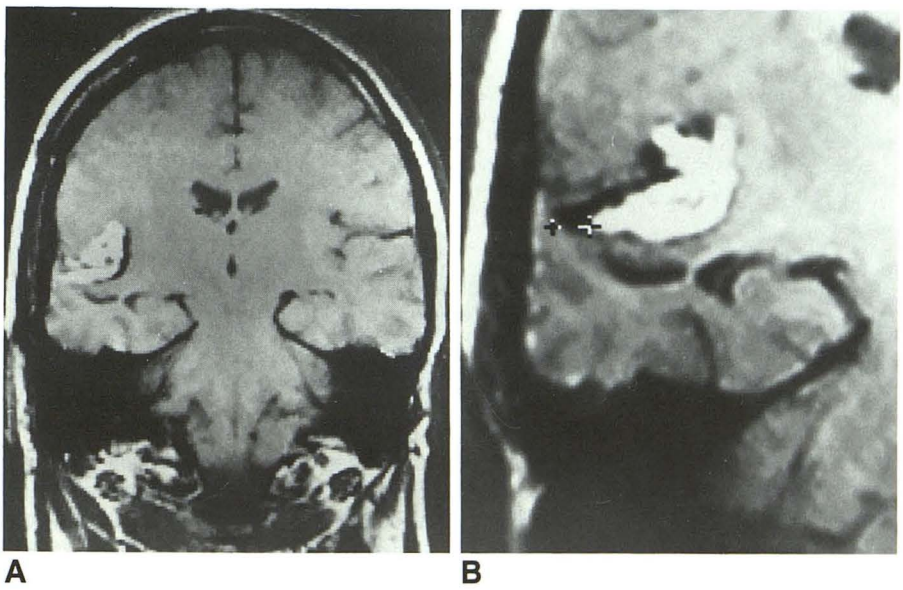

Fig. 6.—Reversal of gradient in frequency-encoded axis (left to right) changes appearance of sylvian fissure lipoma. Dark rim (upfield) part of chemical-shift artifact can mimic signal void of flowing blood or calcification, while bright (downfield) side of artifact structure may hide vessels or calcification.

***A*, Higher gradient to the right.**

***B*, Higher gradient to the left. Signal void at indicated area measures 6 mm, larger than expected 3-mm artifact for system used; it correlated with a vessel at angiography and surgery.**

strength, increasing the bandwidth lessens the distance of the chemical-shift artifact and decreases the signal to noise of the image. The signal to noise of the image is related to bandwidth by the formula, signal to noise = $1/\sqrt{\text{bandwidth}}$. Therefore, an increase in bandwidth from 16 to 32 will decrease the signal to noise by a factor of 1.4 (Table 1).

Sampling bandwidths are inversely proportional to signal collection times. The signal collection time multiplied by the bandwidth (sampling frequency) equals the number of samples (read, × matrix). Therefore, with a constant number of samples, decreasing the sampling bandwidth to improve the signal to noise increases the time required to gather the returning signal and results in an increase in the minimal allowable TE. Asymmetric sampling is a method of data collection that allows a shorter TE without necessitating a change in bandwidth. Traditionally, sampling has been performed in a symmetric distribution around the returning signal. In the spin-echo sequence, after the 180° pulse, the read

TABLE 2: Technical Considerations of Operator-Selectable Bandwidth

Manufacturer/Field Strength	Limiting TE (msec)[a]	Bandwidth (kHz)	Comments
Technicare[b]			
0.6 T (Teslacon II)	43	8.3	–
	28	16.6	–
	20	33.0	Bandwidth is determined by TE and field of view
1.4 T (Teslacon I)	44	8.3	–
	29	16.6	–
	24	33.0	–
General Electric			
1.5 T (Signa)	142	2.0	2- to 32-kHz bandwidth selectable by modifying control variables
	78	4.0	–
	46	8.0	–
	29	16.0	–
	20	32.0	Default setting
Picker International[c]			
0.5 T (Vista)	40 (26)	12.5 (25)	Normal (shorter TE defaults to 25-kHz bandwidth)
	70	6.25	Extended sampling
1.5 T (Vista)	26	25.0	Normal
	60	12.5	Extended sampling

Note.—The selectability of the sampling bandwidth varies by manufacturer, may be run on a default setting, and affects the TE.

[a] Lower TEs are available with fast imaging techniques and asymmetric sampling.

[b] Bandwidth does not change on multiecho sequence.

[c] Bandwidth changes on multiecho sequence.

gradient is turned on while the slice gradient is turned off. Sampling cannot be performed during the interval in which the slice-select gradient is falling off and the read gradient is rising (Fig. 8) [7, 8]. The time between the gradient change and the beginning of signal collection limits how short the TE can be so that sampling does not overlap the gradient change interval. This can be compensated by a wider (higher) bandwidth (Fig. 9). By using asymmetric sampling, the TE can be shorter, allowing a closer spacing of signal collection and gradient change interval without requiring a narrower bandwidth (Fig. 9c).

Table 2 lists the specific parameters for the MR systems we have studied and indicates the degree of TE shortening with changes in sampling bandwidth. It should also be noted that the sampling bandwidth is an operative selectable parameter on the Picker International and General Electric units. If the sampling bandwidth is not selected by the user on these units, the sampling bandwidth will be set by the system (default setting). Default values will yield a high bandwidth, resulting in small chemical-shift artifacts and a shorter allowable TE. Since TE is inversely proportional to bandwidth, if a short TE image is needed to decrease the amount of T2-weighting and increase the amount of T1-weighting or to obtain gradient-recalled images, then a low sampling bandwidth cannot be used. Since chemical-shift artifacts increase with increasing FOV, in areas where a larger FOV is needed, such as the abdomen and pelvis, it is desirable to increase the sampling bandwidth in order to minimize the chemical-shift artifact. If the x matrix is increased, then either the bandwidth or the sampling time must be increased. If the sampling time is increased, the minimal allowable TE will also be increased.

Effect of Chemical-Shift Artifact on Cranial MR

With the Technicare 1.4-T system, the linear distance of chemical-shift artifacts as measured on spin-density-weighted images was 3.2 mm. Therefore, in children under the age of 8, the shift of the signal from fat in the subcutaneous tissues may exceed the average skull thickness and will overlap the brain causing artifactual subdural collection. In the first decade, skull thickness ranges from 2.9 to 3.3 mm, as measured 3 cm posterior to coronal suture [6, 9]. Less commonly between the ages of 8 and 40 and more commonly after age 40, the fat in the diploic space of the calvaria will be shifted over the brain when the distance between the brain and the medullary cavity is less than 3.2 mm. With increasing age, there is increased fat deposition within the marrow, which accounts for the increased prevalence of artifactual subdural hematomas with increasing age. Evaluation of the presence and source of fat signal resulting in subdural hematomas correlated with age-related changes of skull thickness and BPD. Skull thickness increases rapidly up to the teenage years, and then more gradually to age 40 or 50 [9]. The inner table of the skull has a relatively constant thickness of 0.5 mm. Although more variable, the outer table averages 1.5 mm in thickness [6, 10]. Differences in skull thickness are mainly due to the thickness of the diploic space. Between 4 and 20 years of age, the fat cell content of the marrow increases to approximately 21% [11, 12]. Analogous to hemopoietic marrow in other bones of the body, the fat content of the calvarial marrow begins to increase again in the eighth decade [13].

Usually, the appearance of the chemical-shift artifact is so characteristic that it is easily distinguishable from true subdural collections (Fig. 3). The chemical-shift artifact always occurs in the frequency-encoded direction and tapers as the source of fat signal becomes parallel to the frequency axis. Using the same machine and sequence, the frequency offset and apparent subdural location is always on the same side of the brain. Reversal of the direction of the gradient in the frequency-encoded axis results in the artifact being located on the opposite side. This artifact can be mistaken for a true subdural hematoma by those used to working at a different magnetic strength, in systems that alter bandwidth with TE, or when reviewing images from an unfamiliar unit. For questionable subdural hematomas, the phase- and frequency-encoded axes can be reversed or the direction of the gradient strength can be inverted. The dark side of the artifact will add

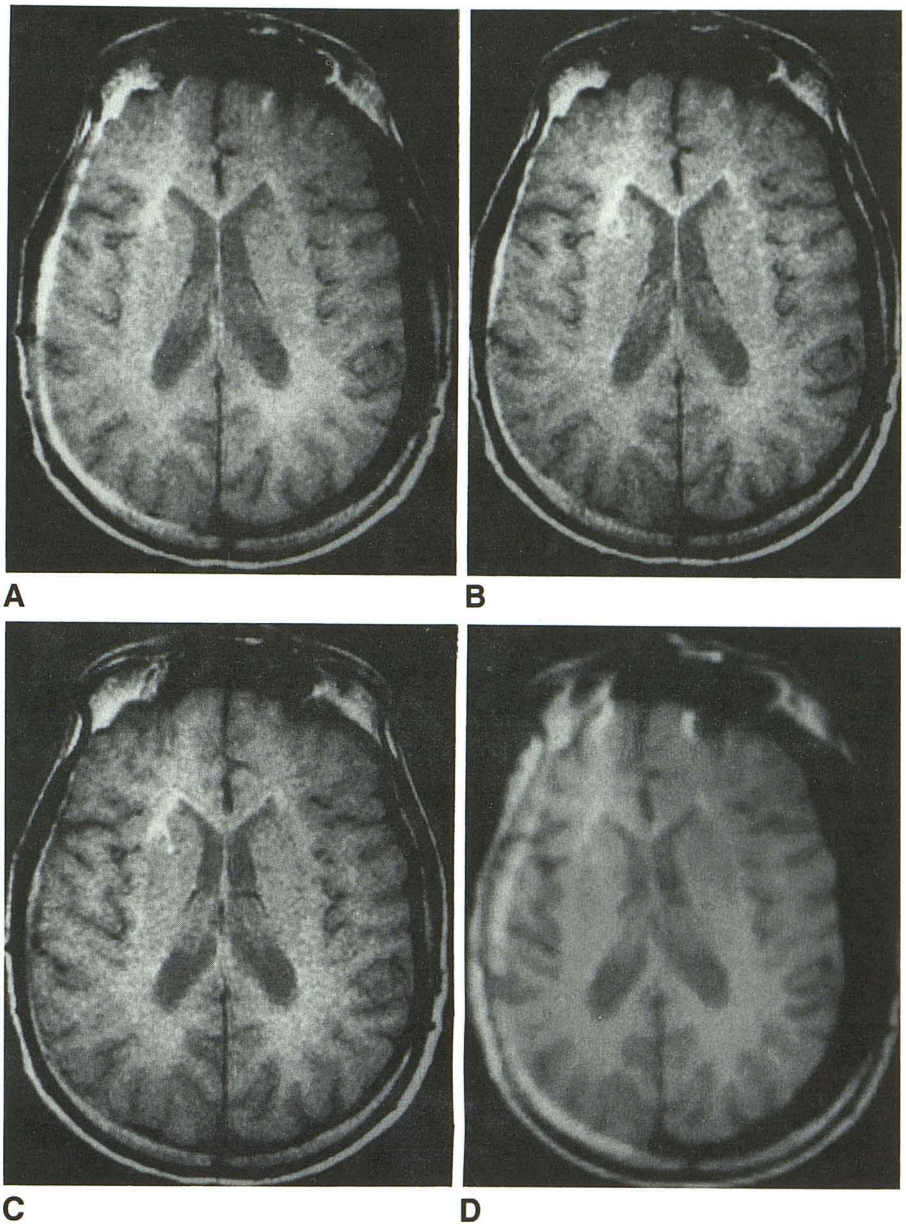

Fig. 7.—Chemical-shift artifact is inversely proportional to sampling bandwidth.
***A–C*, 8- (*A*), 16- (*B*), and 32- (*C*) kHz bandwidths, 500/60 images, 24-cm field of view, 256 × 256 matrix.**
***D*, 8-kHz bandwidth, 48-cm field of view.**

to the signal void of the inner table on the higher gradient side of the skull, and the shift of fat onto the inner table of the lower gradient side adds to the eccentricity of the brain within the halo of fat.

Comparison of CT and MR in the five patients with intracranial lipomas revealed discrete but insignificant apparent location shifts in the lipomas in the downfield direction (Fig. 5). Fat deposits in lipomas of the corpus callosum, interhemispheric fissure, and fat-containing tissues always shifted in the same direction as the subcutaneous fat. An area of decreased signal that may mimic calcification or blood vessels is always adjacent to the lesion in the direction opposite the shift of the fat. In the latter, the dark rim of the chemical-shift artifact is asymmetric and perpendicular to the axis of the frequency-encoded gradient, differentiating it from the concentric ring of decreased signal that surrounds intraparenchymal hemorrhage and represents hemosiderin deposit. Switching the direction of the frequency-encoded gradients or a gradient-echo pulse sequence [14] can be used to determine if calcification is present. The interpretation of the presence of calcifications associated with the intracranial lipomas in this study had no clinical significance. In the case of the sylvian fissure lipoma, deviation in size of the measured vs expected chemical-shift artifact correlated with angiographic and surgical verification of a large vessel. The flow void of the middle cerebral branch artery added to the artifact when the high gradient was to the left and was covered by the signal from the lipoma when the gradient was reversed (Fig. 6).

In conclusion, the relationship of machine-selectable variables on chemical-shift artifacts has been discussed. Chemical-shift artifact is directly proportional to field strength and FOV and inversely proportional to sampling bandwidth. Increasing the bandwidth to compensate for chemical-shift artifacts has consequences in terms of lower signal to noise while allowing a lower minimum TE. Furthermore, chemical-shift artifacts alter brain images in several ways: (1) apparent location shifts of lipomas and other fat-containing tumors, (2) rim artifacts mimicking associated vessels and calcifications while the bright side of the chemical shift can hide such associated structures, and (3) subdural hematomas appearing artifactual. Eccentricity of the brain occurs relative to the halo of subcutaneous fat and diploic fat. The apparent subdural hematomas can result from shift of either subcutaneous or diploic fat. The former occurs in children less than 8 years of age where the distance between brain and subcutaneous fat is less than the linear value of the chemical shift. Increase in the fat content of the enlarged diploic space in adults correlates with the presence of apparent subdural hematomas from the shift of the medullary fat signal across the inner table of the skull.

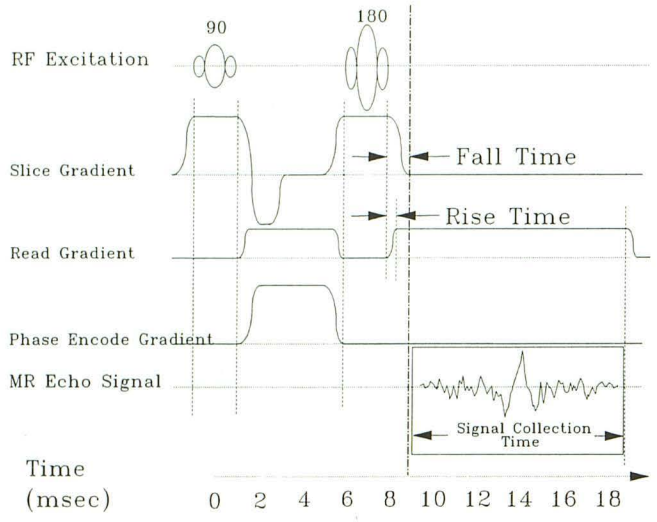

Fig. 8.—Beginning point of data sampling window is controlled by other events in the sequence. *Broken lines* indicate partitions for mutually exclusive events. For the spin-echo sequence, the earliest data sampling (*dot-dash line*) is controlled by falling edge of slice-select gradient, activated during 180° pulse. For other sequences (i.e., gradient echo), dominant factor is rise time of read gradient. These rise and fall times are 100–1500 msec for typical sequences in commercial whole-body MR systems.

ACKNOWLEDGMENTS

We thank Felix W. Wehrli, Hospital of the University of Pennsylvania, Philadelphia, and Linda M. Eastwood and Surya N. Mohapatra, Picker International, Highland Heights, OH, for technical information.

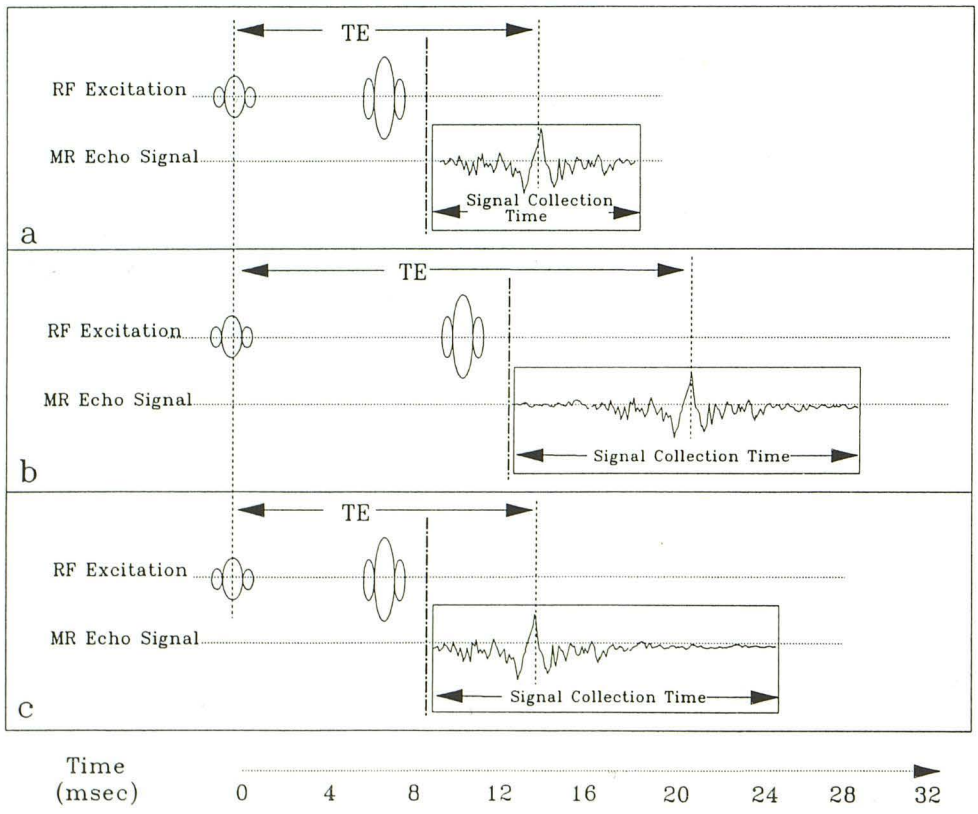

Fig. 9.—Returning echo is sampled at earliest possible interval (*a*). Increasing bandwidth to sample wider range of frequencies and decrease chemical-shift artifact requires a longer TE (*b*), or echo may be sampled asymmetrically (c).

REFERENCES

1. Pople JA, Schneider WG, Bernstein WG. General features of nuclear magnetic resonance spectra. In: Hume DN, King EL, Pope JA, Stork G, Williams HH, Herschbach DR, eds. *High-resolution nuclear magnetic resonance*. New York: McGraw-Hill, **1959**:12–21, 87–91
2. Wehrli FW. *Introduction to fast-scan magnetic resonance*. Milwaukee: General Electric Medical Systems, **1986** (G.E. publication no. 7299)
3. Abraham TJ, Loftus P. In: *Proton and carbon-13 NMR spectroscopy*. London: Heyden, **1979**:Chapter 2
4. Brady TJ, Wismer GL, Buxton R, Stark DD, Rosen BR. Magnetic resonance chemical shift imaging. In: Kressell HY, ed. *Magnetic resonance annual 1986*. New York: Raven, **1986**:55–80
5. Campbell IA, Dwek RA. *Biological spectroscopy*. Menlo Park, CA: Benjamin/Cummings, **1984**:361–367
6. Orley A. *Neuroradiology*. Springfield, IL: Thomas, **1949**:3
7. Provost TJ, Hurst GC. Asymmetric sampling of 2-D FT. Presented at the annual meeting of The Society of Magnetic Resonance in Medicine, Montreal, August **1986**
8. Hendrick RE. Sampling time effect on signal-to-noise, contrast-to-noise. *Magn Reson Imaging* **1987**:5;31–37
9. Adeloye A, Katten KR, Silverman FN. Thickness of normal skull in the American blacks and whites. *Am J Phys Anthopol* **1985**;43:23–30
10. Either R. Thickness and texture. In: Newton TH, Potts DG, eds. *Radiology of the skull and brain*, vol. 1, book 1. St. Louis: Mosby, **1971**:155–157
11. Russel WJ, Yoshinaga H, Antokir SH, Mizuno M. Active bone marrow distribution in the adult. *Br J Radiol* **1966**;39:735–739
12. Ellis RE. Distribution of active bone marrow in the adult. *Phys Med Biol* **1961**;5:255–258
13. Hartsock RJ, Smith EB, Petty CS. Normal variations with aging of the amount of hemapoietic tissue in bone marrow from the anterior iliac crest. *Am J Clin Pathol* **1965**;131:326–333
14. Atlas SW, Grossman RI, Hackney DB, et al. Calcified intracranial lesions: detection with gradient-echo-acquisition rapid MR imaging. *AJNR* **1988**;9:253–259, *AJR* **1988**;150:1383–1389